Theoretical Chemistry Accounts (2021) 140:91
https://doi.org/10.1007/s00214-021-02783-4

REGULAR ARTICLE

Optical properties of $Ag_{29}(BDT)_{12}(TPP)_4$ in the VIS and UV and influence of ligand modeling based on real-time electron dynamics

Rajarshi Sinha-Roy[1,2,3] · Xóchitl López-Lozano[4] · Robert L. Whetten[5] · Hans-Christian Weissker[3,2]

Received: 3 November 2020 / Accepted: 17 May 2021 / Published online: 15 June 2021

Abstract

We study the optical properties of the $Ag_{29}(BDT)_{12}(TPP)_4$ cluster, the geometry of which is available from experimental structure determination, by means of Fourier-transformed induced densities from real-time (time evolution) calculations of time-dependent density-functional theory. In particular, we demonstrate the influence of the ligands on the optical spectra in the visible region and, even more, in the UV. A strong peak in the UV reminiscent of the spectrum of isolated benzene is found to be caused by the phenyl rings of the TPP ligand molecules. Nonetheless, their absence in the modeling also impacts the absorption in the visible region substantially. By contrast, the aromatic rings of the BDT ligands are more strongly coupled to the silver core and loose the character of independent oscillators; they contribute a much less peaked UV absorption. Our results underline the importance of properly accounting for the full ligands for precise and reliable modeling.

Keywords Silver clusters · Optical response · Monolayer-protected clusters · Ligand modeling · TDDFT

1 Introduction

The properties of noble-metal clusters are decisively different from those of the respective bulk metals owing to the confinement to very small sizes. Ranging from clusters of but a few atoms to nanoparticles of a few hundred nanometers in diameter, their study is of great importance for the understanding of fundamental questions concerning the physics of nanostructured metals. Wet-chemically produced monolayer-protected clusters play a particular role because many of them are stabilized in particular geometries which can be determined experimentally by X-ray crystallography. In recent years, total structure determination of a large number of monolayer-protected clusters has been accomplished [1, 2], which provides the basis for the advanced study of their properties and, in particular, of structure-property relations.

The efforts of synthesis and total structure determination of monolayer-protected clusters were initially directed mostly at gold clusters due to the relatively high stability against oxidation and to their biocompatibility in view of applications like biomolecule labeling [3], inhibition of HIV fusion [4], or growth inhibition of bacteria [5].

However, silver clusters are likewise interesting for applications in view of their bactericidal effects [6–8]. They were likewise found to form ligand-protected "ultrastable" nanoparticles [9]. Recently, clusters of 29 silver atoms have been reported by different groups to show special stability and interesting optical properties [10–13]. A water-soluble variant, stabilized with lipoate (LA) ligands and tentatively identified as $Ag_{29}LA_{12}$ by analogy to the hydrophobic homolog

Published as part of the special collection of articles Festschrift in honor of Fernand Spiegelmann.

✉ Hans-Christian Weissker
weissker@cinam.univ-mrs.fr
https://www.etsf.eu

Rajarshi Sinha-Roy
rajarshi.sinha-roy@polytechnique.edu
https://www.etsf.eu

1 Laboratoire des Solides Irradiés, CNRS, CEA/DRF/IRAMIS, École Polytechnique, Institut Polytechnique de Paris, 91128 Palaiseau, France

2 Aix Marseille Univ., CNRS, CINAM, Marseille, France

3 European Theoretical Spectroscopy Facility, https://www.etsf.eu/

4 Department of Physics and Astronomy, One UTSA Circle, The University of Texas at San Antonio, 78249-0697 San Antonio, TX, USA

5 Department of Applied Physics and Materials Science, and MIRA, Northern Arizona University, Flagstaff, Arizona 86011, USA

$Ag_{29}(BDT)_{12}(TPP)_4$ (BDT: 1,3-benzenedithiol; TPP: triphenylphosphine) determined by AbdulHalim et al. [13] has been demonstrated to show antibacterial and antifungal activity [14, 15].

In addition, doping of these 29-atom silver clusters with gold atoms was shown to increase their stability as well as their photoluminescence quantum yield [16]. Calculations of time-dependent density-functional theory (TDDFT) of these gold-doped clusters have been published by Juarez-Mosqueda et al. [17], focusing on the effect of the dopants and analyzing states and optical transitions. However, it appears that a detailed analysis of the pure $Ag_{29}(BDT)_{12}(TPP)_4$ has not been published.

Our present work focuses on the structure-determined cluster of Ref. [13], $Ag_{29}(BDT)_{12}(TPP)_4$. In that publication, it is noted that the cluster in charge state −3 (three additional electrons) corresponds to a super-atom complex (SAC) [18] according to the electron counting rule, with an electron count of $n = 29 - 24 + 3 = 8$, thus corresponding to a shell filling $1S^2|1P^6$ and an expected large gap between the 1P and 1D SAC states. That article also contains a TDDFT calculation for which the phenyl rings of the TPP ligands were replaced by -H groups to save time, justified, according to the authors, by the fact that they are not involved in the frontier orbitals. However, no explicit test of the validity of this procedure for the calculation of the spectra was shown. This example points to a more general question: in most calculations of larger monolayer-protected clusters, a truncation of the ligands was necessary either for computational convenience or due to the absence of precise knowledge about their geometry. However, the effect of these simplifications has mostly not been carefully tested, leading, in some cases, to erroneous interpretation of computational results, as we have shown previously [19]. Some general indications for the case of the $Au_{144}(SR)_{60}$ class of compounds have been given by some of the present authors in Ref. [20] in view of the fine structure in the optical absorption spectra of the clusters [21].

In the present work, we present a systematic study of the electronic structure and the optical response of $Ag_{29}(BDT)_{12}(TPP)_4$ using, in particular, the analysis of the induced density from real-time TDDFT that some of the present authors tested and discussed recently [22]. In addition, we investigate the effect of the reduction of the ligands, comparing in detail the full structure, the structure with the phenyl rings of the TPP ligands cut-off as used in Ref. [13], and a minimal model where all ligands are replaced by H saturation.

2 Models and methods

We started from the experimentally determined coordinates of Ref. [13]. In addition to the full structure (1), we used two reduced models: (2) the structure with the phenyl rings of the TPP ligands cut-off and saturated by H atoms, reducing the ligands to PH_3 (this is the model used in Ref. [13]) and (3) a minimal model where all the rings are replaced by hydrogens, i.e., $Ag_{29}(SH)_{24}(PH_3)_4$. The resulting structures are shown in Fig. 1. In all cases, the charge state -3 was used.

The truncation of the ligands and their replacement by simpler and smaller moieties raises another question: should only the added new parts, in our case the H atoms, be relaxed? Or should the entire structure be relaxed after the replacement? The first solution is motivated by the goal of the calculation. One wants to describe the full cluster with its complete ligands, their simplification is only applied for computational convenience. However, if only the saturating H atoms are relaxed on the fixed rump structure, the resulting structure is not in equilibrium. Moreover, this approach presumes knowledge of the full ligands' coordinates, which is given in our relatively small case, but which is unavailable in many others. By contrast, the second possibility, relaxation of the full structure including all atoms, incurs changes in the structure of even the cluster core, which might cause deviations from the results for the sought-for full cluster. We have, therefore, used and compared both strategies.

The second issue in the description of the clusters is the choice of the approximations within DFT and TDDFT, i.e., the respective exchange-correlation functionals. The arrangement of the organic ligands, in particular, can be expected to be sensitive to the effect of van-der-Waals

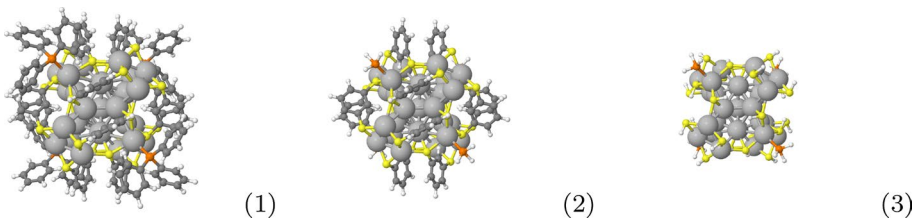

Fig. 1 Structure of the clusters used in the present work: (1) the full structure as taken from the original publication by the Bakr group [13]; (2) the same structure after replacement of the aromatic rings of the TPP ligands by hydrogen atoms as advocated in Ref. [13]; and (3) a minimal model where all the ligands are replaced by hydrogen saturation. (Yellow = sulfur, orange = phosphorus.)

interactions. For the structural relaxations, therefore, we study the effect of incorporating the van-der-Waals interactions as prescribed by Grimme et al. (DFT-D3) [23]. The GGA functional PBE for the exchange-correlation energy is used for all calculations for structure relaxation. In the following, "PBE-D3" refers to using PBE functional in a DFT-D3 calculation.

For the calculation of the optical response it is in particular the description of long-range interactions that must be properly taken care of. For that reason, we use and compare the PBE functional and the asymptotically corrected LB94 functional [24].

The relaxation of the clusters was carried out using the plane-wave code `VASP` [25, 26] using the projector-augmented-wave (PAW) method for the description of the electron–ion interaction [27]. The description uses the artificial periodicity of a supercell system and one **k** point (Γ). The excess charge of the cluster is compensated by a homogeneous background charge. Relaxation was carried out until forces on all relaxed atoms were smaller than 0.007 eV/Å.

The electronic states and the optical spectra have been calculated using DFT and TDDFT with the real-space code `octopus` [28–30]. To this end, using the relaxed structures from the VASP calculation, a ground-state calculation is followed by a time-evolution (real time) TDDFT calculation. Norm-conserving Troullier-Martins pseudopotentials have been used which include the *d* electrons in the valence, that is, with 11 valence electrons for each silver atom. The gradient-corrected PBE exchange-correlation potential and the asymptotically corrected LB94 functional have been used. The real-space grid spacing was set to 0.18 Å, the radius of the spheres around each atom that make up the (non-periodic) calculation domain was set to 5 Å. All calculations are carried out without spin polarization. Therefore, all states are doubly occupied. The projected density of states was obtained from the ground-state wave functions of the `octopus` calculation using the recipe as detailed in Ref. [18]. Details are described in the Supplementary Information.

Optical spectra were calculated using the Yabana-Bertsch time-evolution formalism [31] of TDDFT. The ETRS propagator ("enforced time-reversal symmetry") was used. Propagation time was 25 fs.

In order to analyze the electronic modes contributing to the individual features in the absorption spectra, we used the Fourier-transform analysis of the time-dependent induced density that some of the present authors recently presented and analyzed in detail [22]. The method is briefly described in the Supplementary Information. The time-dependent induced densities for each 25th time-step were used to perform the Fourier transformation at each of the grid points. The grid spacing (0.18 Å), the interval between two consecutive time-steps ($dt = 0.0024\hbar/\mathrm{eV}$) and the total time of evolution (15625*dt) were chosen to be the same as in the `octopus` simulation for the corresponding spectra. A damping of 0.0037 atomic unit of energy (≈0.1 eV) was chosen for the exponential window function during the Fourier transform. The modes of induced density corresponding to optical absorption at a given energy are shown as the Fourier sine coefficients which were written out for 100 equally spaced frequency points between 0 and 0.27 atomic units of energy (≈ 7.35 eV). Graphics of induced densities were prepared with the UCSF Chimera package [32].

3 Results and discussion

To study and quantify the differences incurred by the simplifications of the full ligands, we have analyzed the interatomic distances between the silver atoms in the three relaxed structures for the case when all atoms are relaxed. Most of the Ag-Ag bonds do not change strongly upon removal of the phenyl rings from the TPP ligands, as can be seen in Supplementary Figures S1 and S2 for the PBE and the PBE-D3 relaxations. However, those which are the most directly connected to the P atoms, viz. the sides of the triangular pyramids pointing outward to the silver atoms to which the P atoms are bound, shorten very strongly, from 3.40 to 3.16 Å (PBE-D3) and from 3.58 to 3.18 Å (PBE) (labeled g in Supplementary Figure S1). A similar effect is seen on the 12 bonds pointing outward on the rectangular triangular "towers" labeled f, which shorten strongly upon removal of the BDT ligands.

The electronic and optical properties that we present in the following have been obtained using the following choices: relaxation using PBE-D3 because of its physical motivation, with relaxation of only the saturating H atoms; thereafter, ground-state DFT and TDDFT calculations in octopus using the PBE functional based on the comparison with experiment (see below). The differences with respect to the other possibilities are analyzed at the end of this article.

The electronic structure of the full cluster (1) and of the two simplified models is shown in Fig. 2, the energies of the states around the HOMO-LUMO gap in Supplementary Figure S5. The individual states are shown in Supplementary Figures S6, S7 and S8. We confirm the designation of the cluster as 8-electron super-atom complex. However, in our calculations of the full structure, the three SAC 1P states lie 0.13 eV *below* a group of non-SAC states that constitute the HOMO. The LUMO, by contrast, corresponds indeed to the 1D states.

This situation is not very different in structure (2) after removal of the TPP ligands' phenyl rings, except that one more state approaches the energy of the (non-SAC) HOMO group of states. Finally, the removal of all the rings in the minimal model (3) turns out to represent the essence of the

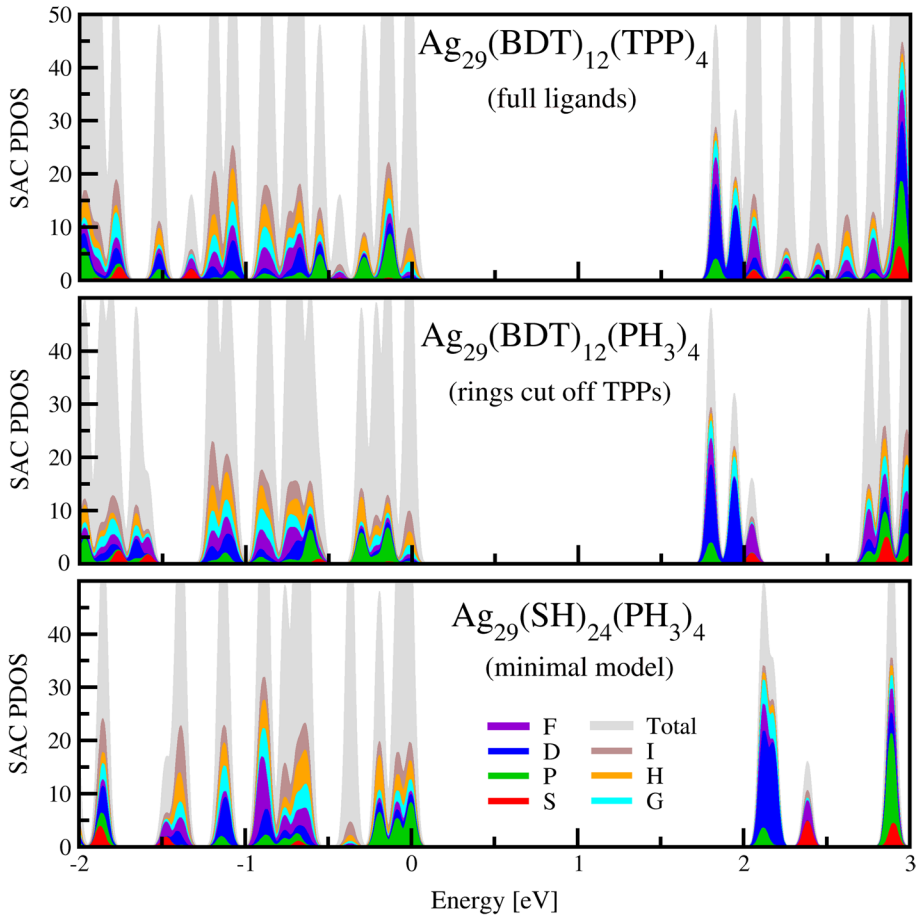

Fig. 2 SAC projected density of states of the full structure (1) with the complete ligands and of the two reduced models (2) and (3). Charge state of -3 in all cases. The zero of the energy axis is the HOMO energy in all cases. Wave functions and energies are from the PBE ground-state calculation in octopus using PBE-D3-relaxed structures

SAC structure: here, the frontier orbitals are indeed the SAC P and D states.

The absorption spectra are shown in Fig. 3. The VIS spectrum of the full structure (1) is characterized by a shoulder at 2.20 eV and three peaks at 2.64, 3.08 and 3.31 eV. In addition, a very strong peak in the UV, at 6.47 eV, is visible. The calculated spectra using the PBE functional agree rather well with experiment below 3 eV, with a small shift of about 0.14 eV, cf., Supplementary figure S4. We note that our result agrees rather well with the spectrum of the pure silver cluster included in Ref. [17].

The spectrum of structure (2) (rings cut off from the TPP ligands) retains a certain similarity to that of the complete structure (1), but the differences even in the lower VIS portion of the spectrum are rather strong. In particular, the intensities of the different peaks are very different. We conclude that the replacement of the rings on the TPP ligands is not an option for the reliable calculation of the spectra in the VIS, in spite of the fact that they do not contribute to the frontier orbitals [13]. In addition, the strong peak at 6.47 eV has almost completely vanished, pointing to the fact that it originates in large part from the TPP phenyl rings, as will be discussed below.

For the minimal model, structure (3), the resemblance with the spectrum of the full structure in the VIS is essentially lost, the spectra are very different and more peaked (doubtless due to the lower number of transitions available). The high-energy peak in the UV is entirely missing and replaced by a background of unspecific absorption.

All these findings point to the importance of the ligands for the optical properties. We will now analyze the respective transitions using our tool of spatially resolved Fourier transform on the induced density from a real-time ("time evolution") TDDFT calculation [22].

In Fig. 4, we show the Fourier-transformed induced densities of the full cluster at 4 energies corresponding to the peaks in the VIS at 2.20, 2.64, 3.08 and 3.31 eV. They show that the three peaks at 2.64, 3.08, and 3.31 eV are mainly due to contributions in the silver "core," although coupled to contributions in the ligands. This includes small but real contributions from the four TPP ligands, which in turn explains well the differences between the spectra of the full structure (1) and the structure (2) where the TPP ligands have been reduced to PH_3. The contributions in the BDT ligands are stronger, which in turn explains the complete change of the spectra if these are

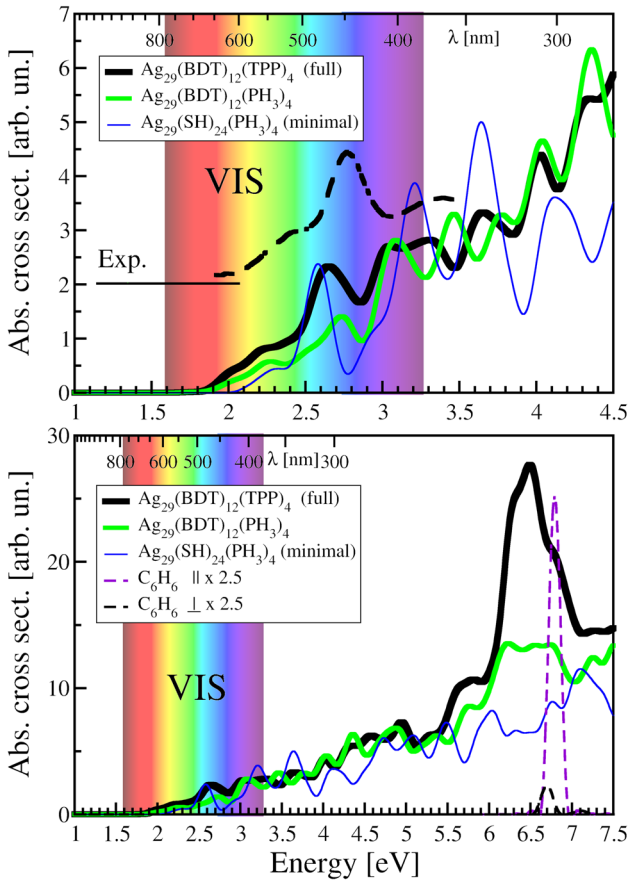

Fig. 3 Spectra of monolayer-protected Ag_{29} calculated for the three structures using real-time TDDFT. We show the VIS part of the spectrum (upper panel) and a wider range including the high-energy peak at 6.47 eV (lower panel). In all cases, PBE-D3 was used for the ionic relaxation, and the PBE functional was used for the optical calculations (including the ground-state calculation preceding the time-evolution calculation). The charge state of -3 was used in all cases. In addition, the spectra of benzene, calculated using the same numerical parameters, are added in the lower panel for excitation perpendicular and parallel to the ring to highlight the similarity of the strong UV peak to the benzene spectrum

removed, as in the minimal model structure (3). The low-energy shoulder at 2.20 eV is clearly due to an excitation in the silver core, with negligible contribution from the ligands, as shown in Fig. 4.

The high-energy UV peak at 6.47 eV is caused principally by the excitation of the ligand rings, which is clearly visible in the iso-surface representation of the induced densities on the left-hand side of Fig. 5. This is also clearly corroborated by the similarity of the high-energy peak to the spectra of pure, isolated benzene as shown in the lower panel of Fig. 3. The iso-surface representation in Fig. 5 shows clearly that *all the rings contribute,* those of the TPP *and* those of the BDT ligands. However, there is clearly a difference, as suggested by the difference in the spectra: after removal of the phenyl rings of the TPP ligands, the high-energy peak of the full cluster (1) is strongly reduced and replaced by a bump in the spectra consisting of a number of low-intensity peaks. The difference between this spectrum of structure (2) and that of the minimal model (3) is due to the contributions of the BDT rings, clearly broadened and deviating from the excitations of the isolated benzene due to strong coupling to the silver "core" of the cluster. Also, the contributions from the aromatic rings of the BDT ligands are weaker than the ones from TPP phenyl rings. This can be clearly seen in the color map representation of the planes in Fig. 5, where the relative values of the induced density around the BDT ligands are much smaller than the values around the phenyl rings of the TPP ligands. We infer from this that the coupling of the BDT rings via the S atoms makes them lose their quality as independent resonators. Indeed, the spectrum between 6 and 7 eV is not strikingly different from that of the minimal structure (3) in which all the aromatic ligand rings have been removed.

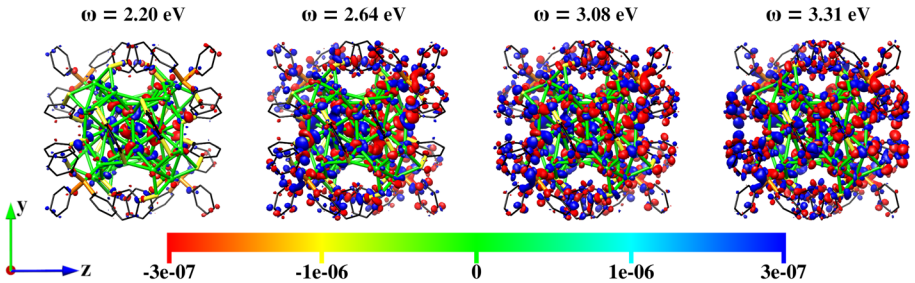

Fig. 4 The Fourier-transformed induced densities in $Ag_{29}(BDT)_{12}(TPP)_4$ at energies (in the VIS) of 2.20, 2.64, 3.08 and 3.31 eV are shown for an iso-surface value of $\pm 3 \times 10^{-7}$ (red and blue), along with the atomic arrangements in the cluster. The perturbation was applied along the z-axis. We show the reconstructed modes at a quarter period, and details are explained in the Supplementary Material

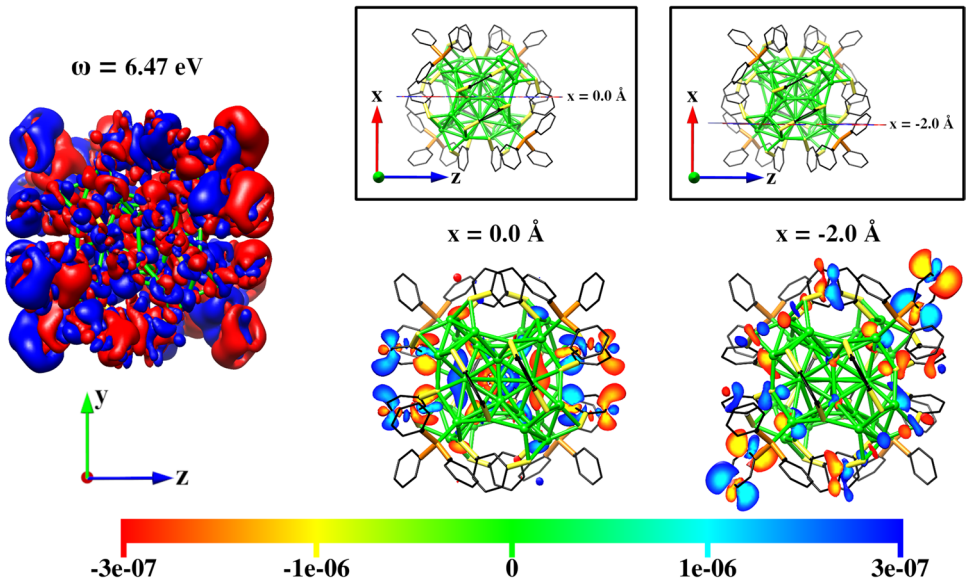

Fig. 5 The Fourier-transformed induced density corresponding to the high-energy UV peak at 6.47 eV in $Ag_{29}(BDT)_{12}(TPP)_4$ is shown (at left) as an iso-surface with $\pm 3 \times 10^{-7}$ iso-value, and as surface color maps for two different planes in the y-z plane, at $x = 0.0$ Å (through the center of the cluster) and $x = -2.0$ Å; the position of the planes is indicated in the framed insets. The plane through the center (at $x = 0.0$) of the cluster does not cut through the rings of the TPP ligands but shows the contribution of the BDT rings. By contrast, the value of $x = -2.0$ Å for the second plane has been chosen to highlight the contribution in the TPP rings. The perturbation is applied along the z-axis. The values for the different colors are shown in the color bar

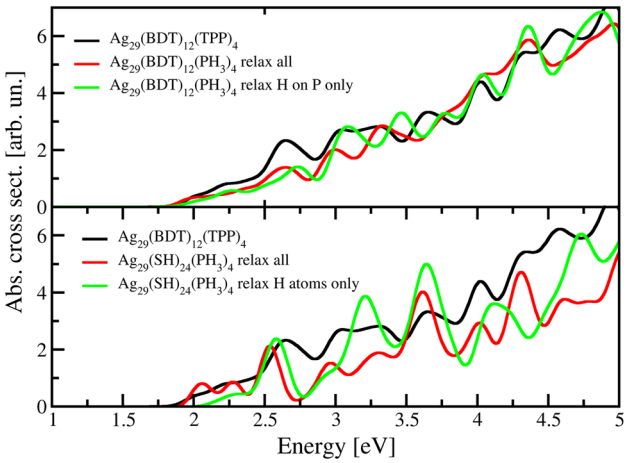

Fig. 6 Effect of relaxing either all atoms or only the saturating H atoms after the truncation of the ligand rings. PBE spectra using PBE-D3-relaxed geometries, the charge state is -3

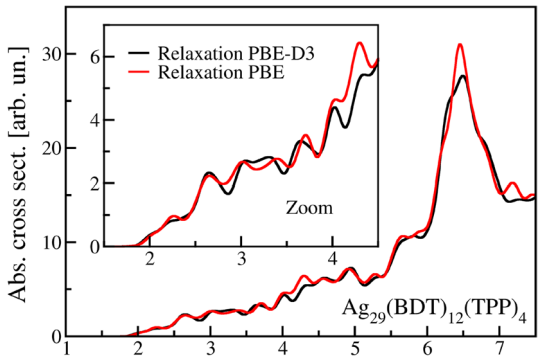

Fig. 7 PBE Spectra for geometries relaxed with inclusion of van-der-Waals corrections (PBE-D3), or without (PBE). The charge state is -3

4 Technical differences

We are now going to discuss the differences produced using the other choices as far as modeling and approximations in TDDFT are concerned. In Fig. 6, we compare the results obtained by relaxing only the saturating H atoms with those obtained by relaxing all atoms. Clearly, there are differences. For the $Ag_{29}(BDT)_{12}(PH_3)_4$ structure, these appear mainly above 2.8 eV. For the minimal model, spectra are very different even at low energies.

We now analyze the differences of spectra calculated for the geometries from relaxation with inclusion of van-der-Waals corrections (PBE-D3), or without (PBE). The structural differences are shown in Supplementary Figures S2 and S3. While this can certainly not be generalized easily, the differences remain relatively small for the cluster we are concerned with, as shown in Fig. 7.

Finally, after obtaining the geometry to be used, the calculation of the optical response needs to be carried out using an appropriate functional as well. In the case of ligand-protected clusters, this choice is difficult because a functional

that would fare well for the metal core would not necessarily work well for the organic ligands at the same time. The simple GGA functional PBE is certainly a compromise. Here, we compare its performance with the asymptotically corrected PB94 functional. The resulting energies and the density of states from the ground-state calculation are compared in Supplementary Figures S3 and S5. We note that the energetic order of the states in the vicinity of the HOMO-LUMO gap changes between the two calculations. While the SAC P states are not the HOMO states for the complete structure in both cases (5 states are slightly higher in energy), the LUMO consists of the SAC D states in the PBE calculation, but a number of other states lie closely below them in the LB94 calculation as can be seen in Supplementary Figure S5.

The spectra are shown in Supplementary Figure S4. The differences in the spectra caused by the two functionals are clearly larger than the ones originating from the inclusion of van-der-Waals interactions in the relaxations, and the PBE spectra are clearly closer to the available experimental res ults.

5 Conclusions

We have carried out an analysis of the optical spectra of $Ag_{29}(BDT)_{12}(TPP)_4^{-3}$ in view of the nature of the excitations and of the influence of the different ligands present in the structure. The customary procedure of truncating the TPP ligands, justified by the assumption that they are not involved in the frontier orbitals, gives a decent description of the states around the HOMO-LUMO gap, but it easily leads to questionable results for the optical spectra in the visible region (and beyond, of course.) We find that the truncation changes some of the silver bonds of the outer part of the silver core strongly if all atoms are allowed to relax. This leads to modifications in the order of the electronic states (Fig. 8).

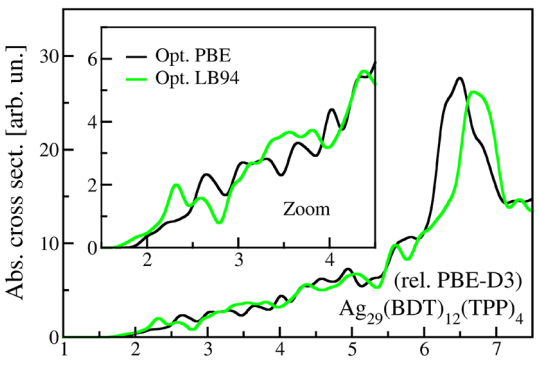

Fig. 8 Calculated spectra (GS + time evolution) using the PBE and the LB94 functionals. In both cases, the PBE-D3-relaxed geometry was used, and the charge state is -3

We have compared different choices applied in our calculations against alternatives: relaxation of all atoms vs. relaxation of the saturating H atoms only; structural relaxation with and without inclusion of van-der-Waals interactions through DFT-D3 calculation; calculation of the optical properties using the simple GGA functional PBE vs. the asymptotically corrected LB94. The latter point caused the biggest differences. The much better agreement with experiment of the PBE spectra compared with the LB94 spectra led us to choose PBE, based on PBE-D3-relaxed structures, for the main comparisons of this work.

The cluster is indeed an 8-electron super-atom complex, but in our calculations, 5 states mostly localized in the ligands are found inside the SAC gap; the HOMO group of states does not consist of SAC states.

We analyzed the excitations that appear in the absorption spectra using spatially resolved Fourier transform of the induced densities of the time-evolution TDDFT calculation. The spectra in the VIS are due to excitations mostly localized in the core but coupled to contributions from the ligands. This coupling is sufficient to render the above-mentioned truncation of the TPP rings inadequate for the description of the spectra in the VIS region. The high-energy UV peak is mainly due to the TPP ligands, their phenyl rings constituting almost independent oscillators. It is strongly diminished when the rings are cut-off. By contrast, the aromatic rings of the BDT ligands are much more strongly coupled to the excitations of the core; their absence changes the spectra entirely even in the visible region. Our analysis shows that for the reliable calculation of even the visible range of optical absorption spectra, the full structure including all parts of the ligands needs to be treated.

Supplementary Information The online version supplementary material available at https://doi.org/10.1007/s00214-021-02783-4.

Acknowledgements We thank Pablo García González for enlightening discussions. This work has been carried out in part thanks to the support of the A*MIDEX grant (n°ANR-11-IDEX-0001-02) funded by the French Government "Investissements d'Avenir" program. We acknowledge support from the French National Research Agency (Agence Nationale de Recherche, ANR) in the frame of the project "FIT SPRINGS", ANR-14-CE08-0009. This work has used HPC resources from GENCI-IDRIS (Grant 2018-096829). Moreover, HCW and RSR would like to acknowledge the contribution of the International Research Network IRN Nanoalloys (CNRS).

References

1. Negishi Y, Nakazaki T, Malola S, Takano S, Niihori Y, Kurashige W, Yamazoe S, Tsukuda T, Häkkinen H (2015) J Am Chem Soc 137(3):1206
2. Jin R, Pei Y, Tsukuda T (2019) Acc Chem Res 52(1):1

3. Ackerson CJ, Powell RD, Hainfeld JF (2010) In: Cryo-EM Part A Sample Preparation and Data Collection, Methods in Enzymology, vol. 481, ed. by G.J. Jensen (Academic Press, 2010), pp 195 – 230
4. Bowman MC, Ballard TE, Ackerson CJ, Feldheim DL, Margolis DM, Melander C (2008) J Am Chem Soc 130(22):6896
5. Bresee J, Maier KE, Boncella AE, Melander C, Feldheim DL (2011) Small 7(14):2027
6. Rai M, Yadav A, Gade A (2009) Biotechnol Adv 27(1):76
7. Ayala-Núñez NV, Lara Villegas HH, del Carmen Ixtepan Turrent L, Rodríguez Padilla C (2009) NanoBiotechnology 5(1):2
8. Lara HH, Garza-Treviño EN, Ixtepan-Turrent L, Singh DK (2011) J Nanobiotechnol 9(1):30
9. Desireddy A, Conn BE, Guo J, Yoon B, Barnett RN, Monahan BM, Kirschbaum K, Griffith WP, Whetten RL, Landman U, Bigioni TP (2013) Nature 501:399
10. Kumar J, Kawai T, Nakashima T (2017) Chem Commun 53:1269
11. van der Linden M, Barendregt A, van Bunningen AJ, Chin PTK, Thies-Weesie D, de Groot FMF, Meijerink A (2016) Nanoscale 8:19901
12. Russier-Antoine I, Bertorelle F, Hamouda R, Rayane D, Dugourd P, Sanader Z, Bonacic-Koutecky V, Brevet PF, Antoine R (2016) Nanoscale 8:2892
13. AbdulHalim LG, Bootharaju MS, Tang Q, Del Gobbo S, AbdulHalim RG, Eddaoudi M, Jiang DE, Bakr OM (2015) J Am Chem Soc 137(37):11970
14. Lopez P, Lara HH, Mullins SM, Black DM, Ramsower HM, Alvarez MM, Williams TL, López-Lozano X, Weissker HC, García AP, Garzón IL, Demeler B, Lopez-Ribot JL, Yacamán MJ, Whetten RL (2018) ACS Appl Nano Materials 1(4):1595
15. Lara HH, Black DM, Moon C, Orr E, Lopez P, Alvarez MM, Baghdasarian G, Lopez-Ribot J, Whetten RL (2019) ACS Omega 4(26):21914
16. Soldan G, Aljuhani MA, Bootharaju MS, AbdulHalim LG, Parida MR, Emwas AH, Mohammed OF, Bakr OM (2016) Angew Chem Int Ed 55(19):5749
17. Juarez-Mosqueda R, Malola S, Hakkinen H (2017) Phys Chem Chem Phys 19:13868
18. Walter M, Akola J, Lopez-Acevedo O, Jadzinsky PD, Calero G, Ackerson CJ, Whetten RL, Grönbeck H, Häkkinen H (2008) Proc Natl Acad Sci 105(27):9157
19. Sinha-Roy R, López-Lozano X, Whetten RL, García-González P, Weissker HC (2017) J Phys Chem C 121(10):5753
20. Weissker HC, Lopez-Acevedo O, Whetten RL, López-Lozano X (2015) J Phys Chem C 119(20):11250
21. Weissker HC, Escobar HB, Thanthirige VD, Kwak K, Lee D, Ramakrishna G, Whetten R, López-Lozano X (2014) Nat Commun 5:3785
22. Sinha-Roy R, García-González P, López Lozano X, Whetten RL, Weissker HC (2018) J Chem Theory Comput 14:6417
23. Grimme S, Antony J, Ehrlich S, Krieg H (2010) J Chem Phys 132(15):154104
24. van Leeuwen R, Baerends EJ (1994) Phys Rev A 49:2421. https://doi.org/10.1103/PhysRevA.49.2421
25. Kresse G, Furthmüller J (1996) Comput Mat Sci 6:15
26. Kresse G, Joubert D (1999) Phys Rev B 59:1758
27. Blöchl PE (1994) Phys Rev B 50:17953
28. Marques MAL, Castro A, Bertsch GF, Rubio A (2003) Comp Phys Comm 151:60
29. Castro A, Marques MAL, Appel H, Oliveira M, Rozzi C, Andrade X, Lorenzen F, Gross EKU, Rubio A (2006) Phys Stat Sol (b) 243:2465
30. Tancogne-Dejean N, Oliveira MJT, Andrade X, Appel H, Borca CH, Le Breton G, Buchholz F, Castro A, Corni S, Correa AA, De Giovannini U, Delgado A, Eich FG, Flick J, Gil G, Gomez A, Helbig N, Hübener H, Jestädt R, Jornet-Somoza J, Larsen AH, Lebedeva IV, Lüders M, Marques MAL, Ohlmann ST, Pipolo S, Rampp M, Rozzi CA, Strubbe DA, Sato SA, Schäfer C, Theophilou I, Welden A, Rubio A (2020) J Chem Phys 152(12):124119
31. Yabana K, Bertsch GF (1996) Phys Rev B 54:4484
32. Pettersen EF, Goddard TD, Huang CC, Couch GS, Greenblatt DM, Meng EC, Ferrin TE (2004) J Comput Chem 25(13):1605